Numerical Simulation of Electromagnetic Wave Propagation using Time Domain Meshless Method*)

Soichiro IKUNO, Yoshihisa FUJITA, Taku ITOH[1)], Susumu NAKATA[2)], Hiroaki NAKAMURA[3)] and Atsushi KAMITANI[4)]

Tokyo University of Technology, Katakura, 1404-1 Hachioji, Tokyo 192-0982, Japan
[1)]*Seikei University, Kichijoji-kitamachi, 3-3-1 Musashino, Tokyo 180-8633, Japan*
[2)]*Ritsumeikan University, Nojihigashi, 1-1-1 Kusatsu, Shiga 525-5062, Japan*
[3)]*National Institute for Fusion Science, Oroshi-cho, 322-6 Toki, Gifu 509-5292, Japan*
[4)]*Yamagata University, Johnan, 4-3-16 Yonezawa, Yamagata 992-8510, Japan*

(Received 9 December 2011 / Accepted 7 March 2012)

The electromagnetic wave propagation in various shaped wave guide is simulated by using meshless time domain method (MTDM). Generally, Finite Differential Time Domain (FDTD) method is applied for electromagnetic wave propagation simulation. However, the numerical domain should be divided into rectangle meshes if FDTD method is applied for the simulation. On the other hand, the node disposition of MTDM can easily describe the structure of arbitrary shaped wave guide. This is the large advantage of the meshless time domain method. The results of computations show that the damping rate is stably calculated in case with $R < 0.03$, where R denotes a support radius of the weight function for the shape function. And the results indicate that the support radius R of the weight functions should be selected small, and monomials must be used for calculating the shape functions.

Keywords: electromagnetic wave propagation, FDTD, meshless method, RPIM

DOI: 10.1585/pfr.7.2406044

1. Introduction

In the Large Helical Device (LHD), the electron cyclotron heating device is used for plasma heating. The electrical power which is made by the gyrotron system transmits to LHD by using long corrugated waveguide. However, it is not clear that the shape of curvature of the waveguide or transmission gain of electromagnetic wave propagation theoretically.

Generally, Finite Difference Time Domain (FDTD) method is applied for electromagnetic wave propagation simulation. FDTD method has provided the solution of Maxwell equation directly. Furthermore, FDTD method has great advantages in terms of parallelization and treatment of problems and so on. However, the numerical domain should be divided into rectangle meshes if FDTD method is applied for the simulation, and it is difficult to treat the problem constructed by arbitrary shapes.

As is well known that the mesh approach does not require finite elements or meshless of a geometrical structure. And various meshless approaches such as the element-free Galerkin (EFG) method and the meshless local Petrov-Galerkin (MLPG) method and the radial point interpolation method (RPIM) have been developed [1, 2]. And these methods are applied to a variety of engineering fields and the fields of computational magnetics. In particular, meshless approaches based on RPIM are applied to time dependent problems [3].

The purpose of the present study is to develop numerical code for analyzing electromagnetic wave propagation in arbitrary shapes of waveguide using meshless approach based on RPIM.

2. Shape Function of Modified RPIM

In the Meshless Time Domain Method (MTDM), the governing equation of the electromagnetic wave propagation phenomenon is discretized by using the shape function of the radial point interpolation method (RPIM). The shape function of RPIM is derived as follows.

First, we scatter N nodes $\boldsymbol{x}_1, \boldsymbol{x}_2, \cdots, \boldsymbol{x}_N$ in the target domain and the boundary, and assign the Radial Basis Function (RBF) $w_1(\boldsymbol{x}), w_2(\boldsymbol{x}), \cdots, w_N(\boldsymbol{x})$ with compact support to the nodes. Then, the solution $u(\boldsymbol{x})$ can be expanded as

$$u(\boldsymbol{x}) = [\boldsymbol{w}(\boldsymbol{x})^T, \boldsymbol{p}(\boldsymbol{x})^T]G^{-1}\begin{bmatrix} \boldsymbol{u} \\ \boldsymbol{0} \end{bmatrix} = \boldsymbol{\phi}(\boldsymbol{x})\boldsymbol{u}, \tag{1}$$

where the vector $\boldsymbol{w}(\boldsymbol{x})$, $\boldsymbol{p}(\boldsymbol{x})$, $\boldsymbol{u}(\boldsymbol{x})$ and $\boldsymbol{\phi}(\boldsymbol{x})$ are defined by

$$\boldsymbol{w}(\boldsymbol{x}) = [w_1(\boldsymbol{x}), w_2(\boldsymbol{x}), \cdots, w_N(\boldsymbol{x})]^T, \tag{2}$$

$$\boldsymbol{p}(\boldsymbol{x}) = [p_1(\boldsymbol{x}), p_2(\boldsymbol{x}), \cdots, p_M(\boldsymbol{x})]^T, \tag{3}$$

author's e-mail: s.ikuno@ieee.org

*) This article is based on the presentation at the 21st International Toki Conference (ITC21).

$$\boldsymbol{u} = [u_1, u_2, \cdots, u_N]^T, \tag{4}$$

$$\boldsymbol{\phi}(\boldsymbol{x}) = [\phi_1(\boldsymbol{x}), \phi_2(\boldsymbol{x}), \cdots, \phi_N(\boldsymbol{x})]^T, \tag{5}$$

where $\phi_i(\boldsymbol{x})$ denotes a shape function on $i-$th node. The components of the vector $\boldsymbol{p}(\boldsymbol{x})$ are monomials of the space variables. For example, $\boldsymbol{p}(\boldsymbol{x})^T = [1, x, y]$ and $\boldsymbol{p}(\boldsymbol{x})^T = [1, x, y, x^2, xy, y^2]$ are monomials for the linear and the quadratic approximation. Furthermore, the matrix G is defined by following equation.

$$G = \begin{bmatrix} W & P \\ P^T & O \end{bmatrix}. \tag{6}$$

Here, the matrices W and P are defined by following equations.

$$W = [\boldsymbol{w}(\boldsymbol{x}_1), \boldsymbol{w}(\boldsymbol{x}_2), \cdots, \boldsymbol{w}(\boldsymbol{x}_n)]^T, \tag{7}$$

$$P = [\boldsymbol{p}(\boldsymbol{x}_1), \boldsymbol{p}(\boldsymbol{x}_2), \cdots, \boldsymbol{p}(\boldsymbol{x}_n)]^T. \tag{8}$$

Under the above assumptions, the shape function and its derivative can be expressed as

$$\phi_k(\boldsymbol{x}) = \sum_{i=1}^{N} w_i(\boldsymbol{x}) g_{i,k} + \sum_{j=1}^{M} p_j(\boldsymbol{x}) g_{N+j,k}, \tag{9}$$

$$\frac{\partial \phi_k}{\partial x} = \sum_{i=1}^{N} \frac{\partial w_i(\boldsymbol{x})}{\partial x} g_{i,k} + \sum_{j=1}^{M} \frac{\partial p_j(\boldsymbol{x})}{\partial x} g_{N+j,k}, \tag{10}$$

$$\frac{\partial \phi_k}{\partial y} = \sum_{i=1}^{N} \frac{\partial w_i(\boldsymbol{x})}{\partial y} g_{i,k} + \sum_{j=1}^{M} \frac{\partial p_j(\boldsymbol{x})}{\partial y} g_{N+j,k}, \tag{11}$$

where, $g_{i,j}$ denotes the (i, j) element of matrix G^{-1}. Note that the shape function satisfy the Kronecker delta function property, i.e.

$$\phi_i(\boldsymbol{x}_j) = \begin{cases} 1, & i = j, \\ 0, & i \neq j. \end{cases} \tag{12}$$

In RPIM, the local domain Ω_i for the shape function ϕ_i is selected by using domain of influence of RBF as shown in Fig. 1 (a). From this reason, the matrix G must be calculated for each local domain, and it takes much CPU time to derive the shape functions [2]. On the other hand, modified RPIM has the advantages that the matrices G^l for Ω_l can be calculated prior for the shape function of inside of local domain Ω_l (see Fig. 1 (b)). In the present study, the shape function derived from MRPIM is adopted for the computation [4].

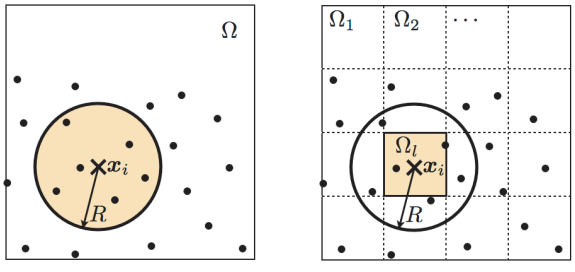

(a) (b)

Fig. 1 The method for selecting the local domain Ω_i for the shape function ϕ_i. (a): RPIM, (b): MRPIM.

3. Meshless Time Domain Method

In the present study, 2D electromagnetic wave propagation of TM mode is adopted for the evaluation. The governing equation of the problem is defined by

$$\varepsilon \frac{\partial E_z}{\partial t} = -\sigma E_z + \frac{\partial H_y}{\partial x} - \frac{\partial H_x}{\partial y}, \tag{13}$$

$$\mu \frac{\partial H_x}{\partial t} = -\frac{\partial E_z}{\partial y}, \tag{14}$$

$$\mu \frac{\partial H_y}{\partial t} = \frac{\partial E_z}{\partial x}, \tag{15}$$

where, H_x and H_y denote the magnetic field of x and y component, and E_z denotes the electric field of z component. In addition, ε, σ and μ denote permittivity, permeability and electroconductivity, respectively.

First, the system is discretized with respect to time by applying Leap Frog Method, and it is transformed to following equations.

$$\frac{\varepsilon}{\Delta t}\left(E_z^{n+1} - E_z^n\right) + \sigma E_z^{n+1/2} = \frac{\partial H_y^{n+1/2}}{\partial x} - \frac{\partial H_x^{n+1/2}}{\partial y}, \tag{16}$$

$$\frac{\mu}{\Delta t}\left(H_x^{n+1/2} - H_x^{n-1/2}\right) = -\frac{\partial E_z^n}{\partial y}, \tag{17}$$

$$\frac{\mu}{\Delta t}\left(H_y^{n+1/2} - H_y^{n-1/2}\right) = \frac{\partial E_z^n}{\partial x}. \tag{18}$$

As we mentioned above, the shape function of RPIM has the Kronecker delta function property (12). By using the shape function and the property, the system can be discretized with respect to space as follows.

$$E_{z,i}^{n+1} = \alpha \left[\left(\frac{\varepsilon}{\Delta t} - \frac{\sigma}{2} \right) E_{z,i}^n + \sum_{j=1}^{N} H_{y,j}^{n+1/2} \frac{\partial \phi_j}{\partial x} - \sum_{j=1}^{N} H_{x,j}^{n+1/2} \frac{\partial \phi_i}{\partial y} \right], \tag{19}$$

$$H_{x,i}^{n+\frac{1}{2}} = H_{x,i}^{n-\frac{1}{2}} - \frac{\Delta t}{\mu} \sum_{j=1}^{N} E_{z,j}^n \frac{\partial \phi_j}{\partial y}, \tag{20}$$

$$H_{y,i}^{n+\frac{1}{2}} = H_{y,i}^{n-\frac{1}{2}} + \frac{\Delta t}{\mu} \sum_{j=1}^{N} E_{z,j}^n \frac{\partial \phi_j}{\partial x}. \tag{21}$$

Here, parameter α is defined as following equation.

$$\alpha = \frac{1}{\frac{\varepsilon}{\Delta t} + \frac{\sigma}{2}}. \tag{22}$$

Note that, the average of $E_{z,i}^n$ and $E_{z,i}^{n+1}$ is adopted for $E_{z,i}^{n+1/2}$. By solving (19), (20) and (21) in each time step, we can obtain the result that describes the behavior of the electromagnetic wave propagation in various shape of wave

Table 1 The geometrical and the physical parameters.

Shape of source wave	sine wave
Amplitude of source wave	1.0 V/m
Frequency of source wave	1.0×10^9 Hz
Speed of wave	299,792,458 m/s
Number of layer for PML	16
Reflectivity coefficient of PML	-80 dB

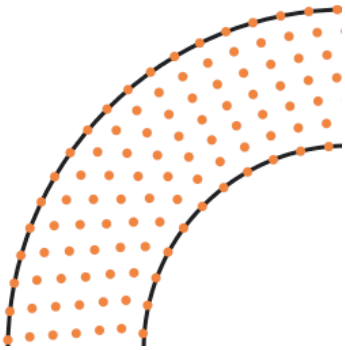

Fig. 2 The conceptual diagram of node structure in curved wave guide.

guide. In addition, the Perfectly Matched Layer (PML) and the Perfect Magnetic Conductor (PMC) are used for absorbing boundary condition and boundary condition.

4. Numerical Evaluation

4.1 Electromagnetic wave propagation in arbitrary shaped wave guide

In this paper, the geometrical and the physical parameters are fixed as Table 1.

First, we show the conceptual diagram of node structure in curved wave guide is shown in Fig. 2. It is very difficult to evaluate the electromagnetic wave propagation in arbitrary shaped wave guide by using the standard FDTD method because FDTD method is generally calculated on orthogonal mesh. And the mesh size becomes small to describe the structure of arbitrary shaped wave guide. On the other hand, the node disposition of MTDM can easily describe the structure of arbitrary shaped wave guide as shown in Fig. 2. This is the large advantage of MTDM compare to the standard FDTD method.

Next, we calculate the behavior of the electromagnetic wave propagation in various shape of wave guide, and the analytic model of the calculation is shown in Fig. 3. We assume that the sides of the wave guide are surrounded by perfect magnetic conductor (PMC), and the absorbing boundary condition is imposed on both end of wave guide. As we mentioned above, the perfectly matched layer (PML) is adopted for the condition. The distributions of electric field E_z in S-shaped wave guide and U-shaped wave guide are shown in Fig. 4. We see from these figures that the distributions of electric field E_z in various shaped

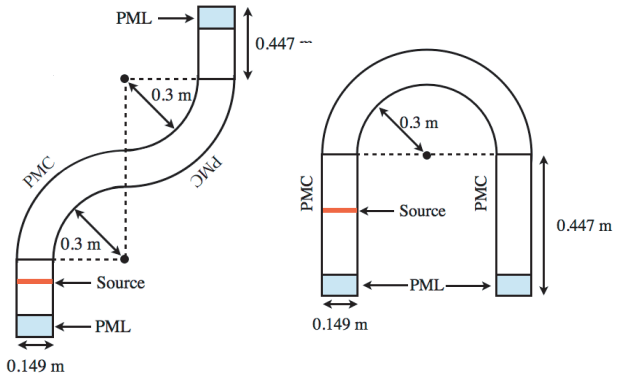

Fig. 3 Analytic domain of S-shaped wave guide and U-shaped wave guide.

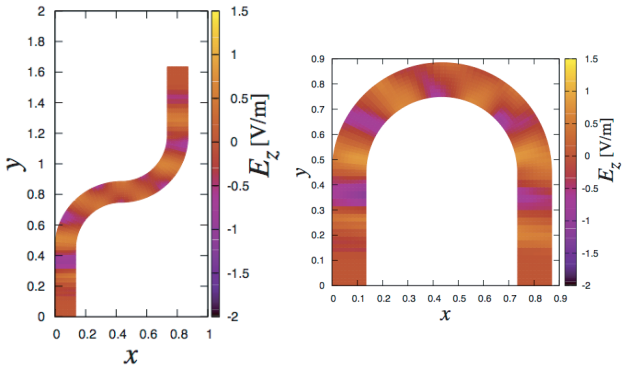

Fig. 4 The distribution of electric field E_z in S-shaped and U-shaped wave guide.

wave guide are calculated clearly, and the distributions of electric field E_z can be observed in each time step.

4.2 Evaluation of shape functions

In the present study, following three types of weight function are adopted for (7).

$$w(r) = e^{-c_1\left(\frac{r}{R}\right)^2}, \tag{23}$$

$$w(r) = 1.0 - 6.0\left(\frac{r}{R}\right)^2 + 8.0\left(\frac{r}{R}\right)^3 - 3.0\left(\frac{r}{R}\right)^4, \tag{24}$$

$$w(r) = (r^2 + R^2)^{-0.5}. \tag{25}$$

Here, r is defined by $r = |\boldsymbol{x} - \boldsymbol{x}_i|$, and R denotes a support radius of the weight function. Besides, c_1 denotes a parameter. The influence of the weight function for the shape function on damping rate is investigated in this section. The analytic model and the distribution of electric field E_z in line shaped wave guide for the evaluation is shown in Fig. 5.

The damping rate R_D in line shaped wave guide is plotted as the function of support radius R in Fig. 6 and Fig. 7. The value of damping rate R is calculated by using

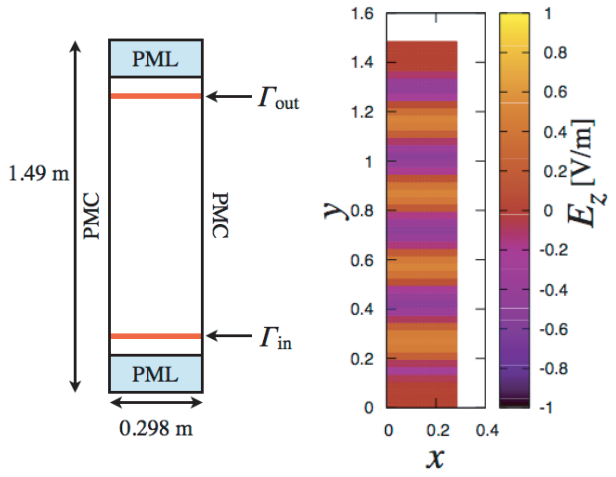

Fig. 5 Analytic domain of line shaped wave guide and the distribution of electric field E_z in line shaped wave guide. Γ_{in} and Γ_{out} denote source input line and observation line, respectively.

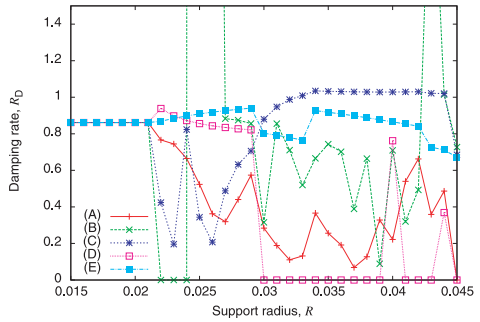

Fig. 6 The damping rate R_D in line shaped wave guide is plotted as the function of support radius R. Note that the no monomial basis is used for calculation of shape function. Here, (A): Eq. (23) with $c_1 = 0.1$, (B): Eq. (23) with $c_1 = 1.0$, (C): Eq. (23) with $c_1 = 5.0$, (D): Eq. (24), (E): Eq. (25).

following equation.

$$R_D = \int_{\Gamma_{out}} E_z \, dl \; / \; \int_{\Gamma_{in}} E_z \, dl. \tag{26}$$

Here, Γ_{in} and Γ_{out} denote a source input line and observation line, and the values of R_D have been calculated on the value of E_z past the line Γ_{out} in a certain time step. We can see from Fig. 6 that the values of damping rate R_D are less than 1.0 even if the support radius is small. Moreover, the values of R_D diverge in case of $R > 0.02$ or unstable behaviors are observed.

On the other hand, the values of damping rate R_D in Fig. 7 are stably calculated and $R_D \neq 1.0$ in case with $R < 0.03$. These results indicate that the support radius R of the weight functions should be selected small, and monomials $\boldsymbol{p}(\boldsymbol{x})$ must be used for calculating the shape functions.

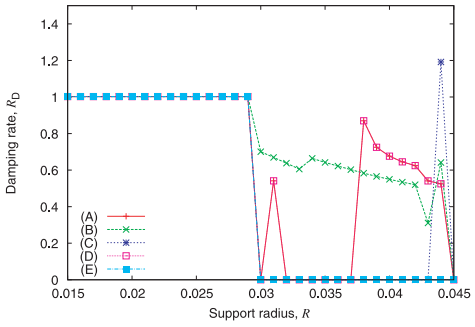

Fig. 7 The damping rate R_D in line shaped wave guide is plotted as the function of support radius R. Note that the linear monomial basis (i.e. $\boldsymbol{p}(\boldsymbol{x}) = [1, x, y]^T$) is used for calculation of shape function. Here, (A): Eq. (23) with $c_1 = 0.1$, (B): Eq. (23) with $c_1 = 1.0$, (C): Eq. (23) with $c_1 = 5.0$, (D): Eq. (24), (E): Eq. (25).

5. Conclusion

We have developed the numerical simulation code for the electromagnetic wave propagation in various shaped wave guide. In addition, we have evaluated the influence of the weight function for the shape function on damping rate of the wave guide.

Conclusions obtained in the present study are summarized as follows.

- The node disposition of MTDM can easily describe the structure of arbitrary shaped wave guide. This is the large advantage of MTDM compared to the standard FDTD method.
- The distributions of electric field E_z in various shaped wave guide are calculated clearly, and the distributions of electric field E_z can be observed in each time step by means of the MTDM code.
- The support radius R of the weight functions should be selected small, and monomials must be used for calculating the shape functions.

Acknowledgment

This work was supported in part by Japan Society for the Promotion of Science under a Grant-in-Aid for Scientific Research (B) No.22360042. A part of this work was also carried out under the Collaboration Research Program at National Institute for Fusion Science, Japan.

[1] T. Belytschko, Y.Y. Lu and L. Gu, Int. J. Numer. Methods Eng. **37**(2), 229 (1994).
[2] J.G. Wang and G.R. Liu, Int. J. Numer. Methods Eng. **54**(11), 1623 (2002).
[3] T. Kaufmann, C. Fumeaux and R. Vahldieck, 24th International Review of Progress in Applied Computational Electromagnetics (ACES 2008) p.426.
[4] S. Nakata, J. Numer. Anal. Indust. Appl. Math. **4**(3-4), 192 (2009).